symmetry

IMPACT FACTOR 2.2

CITESCORE 5.4

Article

# Design of Ranging Communication Coding and Noise Suppression Methods in Space Gravitational Wave Detection

Hongyu Long, Tao Yu, Ke Xue and Zhi Wang

MDPI

https://doi.org/10.3390/sym17010040

*symmetry*

MDPI

*Article*

# Design of Ranging Communication Coding and Noise Suppression Methods in Space Gravitational Wave Detection

**Hongyu Long [1], Tao Yu [1,2,*], Ke Xue [1] and Zhi Wang [1]**

[1] Changchun Institute of Optics, Fine Mechanics and Physics, Chinese Academy of Sciences, Changchun 130033, China; longhongyu@ciomp.ac.cn (H.L.); xuekeciomp@163.com (K.X.); wz070611@126.com (Z.W.)
[2] School of Electronic Information Engineering, Changchun University of Science and Technology, Changchun 130022, China
* Correspondence: yut@ciomp.ac.cn

**Abstract:** A ranging communication system is a key technology for achieving precise ranging and scientific data exchange in space gravitational wave detection, with the aim of realizing the symmetry of interferometer arms. This system is integrated into the phase measurement payload, the 'phasemeter'. Achieving high-ranging accuracy and low-bit error rate communication while mitigating the impact of phase noise has become a focus of current research. This paper starts with the coding methods for ranging communication and analyzes phase modulation noise based on Binary Phase Shift Keying (BPSK). The study found that the main lobe phase noise caused by BPSK modulation is approximately 158 $\mu rad/\sqrt{Hz}$, which is two orders of magnitude higher than the phase-tracking criteria for gravitational wave detection. To address this, this paper proposes a Bit-Balanced Code (BBC) sequence design and optimization method aimed at eliminating main lobe noise. The experimental results show that the optimized BBC sequence improves the metrics of even autocorrelation, odd autocorrelation, maximum spectral amplitude, and even cross-correlation by 7.17, 2.83, 1.22, and 7.16, respectively, compared to the original sequence. Furthermore, experiments have demonstrated that the BBC sequence is insensitive to random data and can achieve dynamic bit balancing to eliminate the DC component. The proposed BBC sequence design method can serve as a reference for technologies related to space gravitational wave detection.

**Keywords:** space gravitational wave detection; ranging communication; bit-balanced code (BBC); phase noise; binary phase shift keying (BPSK)



Received: 28 November 2024
Revised: 21 December 2024
Accepted: 25 December 2024
Published: 28 December 2024

**Citation:** Long, H.; Yu, T.; Xue, K.; Wang, Z. Design of Ranging Communication Coding and Noise Suppression Methods in Space Gravitational Wave Detection. *Symmetry* **2025**, *17*, 40. https://doi.org/10.3390/sym17010040



## 1. Introduction

In the 1990s, the European Space Agency (ESA) and the National Aeronautics and Space Administration (NASA) proposed the Laser Interferometer Space Antenna (LISA) project, aimed at detecting gravitational waves through space-based laser interferometry. With interferometer arms extending millions of kilometers, LISA is capable of effectively detecting gravitational wave sources in the frequency range of 0.1 mHz to 1 Hz, which is crucial for studying the growth and evolutionary history of supermassive black holes in galactic centers and their host galaxies. As a result, space-based gravitational wave detection has attracted widespread attention. In light of this, China formed a working group for space gravitational wave detection in 2008 to conduct related research [1–3].

Currently, both the LISA and China's Taiji program employ a three-satellite system. Using laser heterodyne interferometry, the distance variations between the test masses on

different satellites caused by gravitational waves are converted into phase changes in the interferometric signal, thereby enabling high-precision distance measurements. However, in an actual space environment, the satellites experience relative orbital motion, resulting in a lack of symmetry in the interferometric arm lengths. This causes laser frequency noise, as the frequency jitter of the laser is proportional to the arm length difference. Such frequency noise is one of the main noise sources in space-based gravitational wave detection. To suppress this noise, a three-level technique is typically employed, including frequency stabilization (Pound-Drever-Hall), arm-locking, and Time Delay Interferometry (TDI). These methods reduce the laser frequency instability noise to the order of $10^{-6}$ $Hz^{1/2}$, meeting the detection requirements. This is essentially achieved through inter-satellite ranging and time synchronization, creating an equivalent equal-arm interferometer [3–7].

Therefore, ranging and communication technologies are employed in space gravitational wave detection to achieve inter-satellite distance measurement while simultaneously enabling scientific data exchange, thereby generating an equivalent equal-arm interferometer. The principle is based on spread spectrum communication, where the Pseudo-Random Noise (PRN) ranging code sequence is combined with communication data through an XOR operation to generate the ranging communication code. This ranging communication code is then modulated onto the laser phase using BPSK and transmitted to a remote satellite. Unlike conventional inter-satellite communication and satellite navigation communication, the modulation depth of the ranging communication code in the laser phase is limited to only 0.1 rad to minimize its impact on gravitational wave detection signals. Additionally, space gravitational wave detection integrates the ranging communication system into the critical phase measurement payload, the "phasemeter", necessitating the consideration of the effects of phase modulation on phase measurement [8–10]. According to the integrated study of ranging communication for space gravitational wave detection by Yamamoto [11], if the PRN (bipolar) is unbalanced (i.e., this means that in the sequence, the number of binary values "1" and "−1" is not equal, resulting in an imbalance in their occurrences) or remains unbalanced after combining with data, it will generate a DC component during BPSK modulation, leading to main lobe noise. This will affect the tracking accuracy of the phase signal and cause errors in the ranging accuracy [11]. Currently, both domestically and internationally, there is limited research on noise issues caused by the balance of PRN codes [12,13]. Therefore, this paper analyzes the impact of the balance of PRN codes and presents a method for generating a bit-balanced PRN code that ensures balance in PRN codes of any length occupied by data. Next, core parameters, such as odd-even autocorrelation/cross-correlation functions and maximum spectral amplitude, are used to construct the evaluation criteria. By employing models such as divide-and-conquer path planning and the maximum clique model, the bit-balanced ranging pseudocode sequence with the best overall performance is selected. The method proposed in this paper can effectively eliminate the impact of DC phase noise caused by BPSK modulation, enhancing the robustness of inter-satellite ranging communication in space gravitational wave detection, thereby meeting the requirements for high-precision and high-reliability communication. Meanwhile, this paper provides new ideas and methods for ranging communication coding designs in this field.

The structure of the content of this paper is arranged as follows:

Chapter 2 will provide a detailed analysis of the phase noise caused by BPSK modulation. Through theoretical derivation and mathematical modeling, it will determine the main lobe and sidelobe noise levels in BPSK modulation, aiming to reveal the significant impact of BPSK phase modulation on system noise and emphasize the necessity of optimization in the design;

Chapter 3, in order to suppress the noise caused by BPSK phase modulation, proposes a BBC sequence design and optimization method based on Weil sequences. This method ensures bit balance in PRN sequences of any length during the data encoding process, effectively eliminating the impact of the DC component;

Chapter 4 compares the optimized BBC sequence with the original Weil sequence based on performance indicators, such as odd/even autocorrelation, odd/even cross-correlation, and maximum spectral amplitude. It also analyzes the DC component after modulating the BBC sequence. Through these comparisons, the effectiveness of the optimized BBC sequence design is validated;

In the final chapter, this paper summarizes the research work and discusses the current limitations and future research directions.

## 2. Modulation Phase Noise Analysis

Currently, the inter-satellite absolute position measurement and data communication systems of programs like LISA and Taiji are integrated into the overall laser interferometry system, as shown in Figure 1 [14]. This system exhibits symmetry and is capable of performing functions such as interferometric measurements, inter-satellite communication, and clock noise transfer. The main principle is as follows: independent lasers (referred to as Laser 1 and Laser 2) are installed on the designated master and slave satellites. The master satellite sends a laser to the slave satellite, and after it is reflected by test mass 2 on the slave satellite, it interferes with Laser 2. The resulting signal is then transmitted through a Trans Impedance Amplifier to a Quadrant Photoelectric Detector (QPD), which converts it into an electrical signal. The phase difference between Laser 2 and the received Laser 1 is measured by a phase meter. Weak-light phase locking is used for differential frequency locking, allowing Laser 2 to carry the phase information of the received Laser 1. The phase information is then encoded into the PRN sequence via an Electro-Optic Modulator and modulated onto the laser phase. The locked Laser 2 is then transmitted back to the master satellite. After passing through the same process at the master satellite, the laser interferometric signal containing the inter-satellite test mass distance variation information is obtained. Finally, the phase meter on the master satellite measures the phase change, which is used to calculate the distance variation between the test masses caused by the gravitational wave.

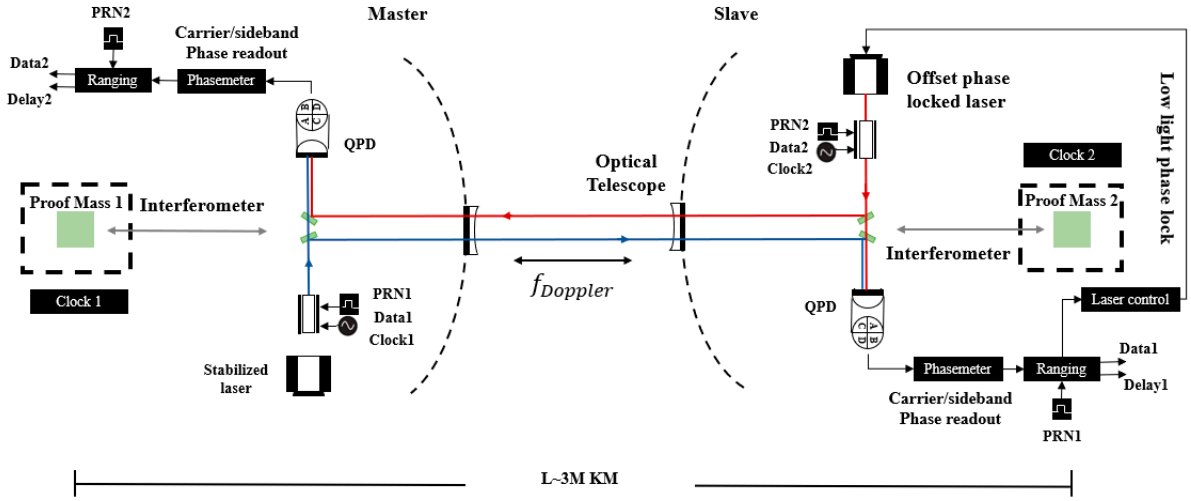


**Figure 1.** Space Gravitational Wave Inter-Satellite Ranging and Communication System.

In the above process, the laser heterodyne interference signal is finally input into a single quadrant of the QPD on the master satellite. Under ideal conditions, it can be represented as [15]:

$$\begin{aligned} V = {} & G_t J_0^2(m_{sb}) \cos[2\pi(f_{main} + f_D)t + \varphi_{main} + m_{prn} \sum_{-\infty}^{\infty} c_n p(t - nT_c)] \\ & + G_t J_1^2(m_{sb}) \cos[2\pi(f_{up} + f_D)t + \varphi_{up}] \\ & + G_t J_1^2(m_{sb}) \cos[2\pi(f_{down} + f_D)t + \varphi_{down}] \end{aligned} \tag{1}$$

$G_t = \frac{\eta G_{TIA}\sqrt{\gamma P_S P_L}}{N}$ represents the total gain of the Trans-Impedance Amplifier (TIA), where $G_{TIA}$ is the TIA gain, $P_S$ and $P_L$ are the received signal power, and the local laser power, $\gamma$ is the heterodyne detection efficiency, and $N$ is the number of photodiodes (QPD: $N$ = 4). $J_n(m)$ denotes the nth-order Bessel function and $m_{sb}$ is the frequency modulation index, approximately 0.45 rad. The control index under this modulation function takes the $J_0$ and $J_1$ terms. $f_{main}$, $f_{up}$ and $f_{down}$ represent the main frequency and the upper and lower frequencies, respectively. $f_D$ refers to the Doppler frequency shift, and $\varphi_{main}$, $\varphi_{up}$ and $\varphi_{down}$ correspond to the phase shifts of the main, upper, and lower frequencies, respectively. The PRN code modulation index $m_{prn}$ is approximately 0.1 rad, and $c_n$ represents the PRN code in binary form, its pulse shape as $p(t)$, and $T_c$ is the period.

From Equation (1), it can be seen that under ideal conditions, the interference signal is only affected by the Doppler shift. However, in actual PRN modulation, BPSK phase modulation generates additive noise in the main and side lobes, which is superimposed on the phase of the main wave beat frequency signal, thus affecting the phase-tracking and locking accuracy. The main lobe noise is caused by the DC component generated by an unbalanced PRN code (with unequal numbers of 1 s and −1 s) during PRN modulation, while the sidelobe noise arises from the incomplete energy concentration in the main lobe and the clock sideband modulation during PRN modulation.

The phase noise $\delta\widetilde{\varphi}_{PRN}(f)$ caused by modulation can be estimated and represented based on the PRN amplitude spectral density $\widetilde{A}_{PRN}(f, f_{het})$ and the root mean square (RMS) of the signal amplitude $A_{het,rms}$ [11].

$$\delta\widetilde{\varphi}_{PRN}(f) = 2\sqrt{2} \cdot \frac{\widetilde{A}_{PRN}(f, f_{het})}{A_{het,rms}} \tag{2}$$

In the equation, $f$ represents the observation band frequency, and $f_{het}$ denotes the heterodyne beat frequency.

The estimation model $\delta\widetilde{\varphi}_{BPSK,main}(f)$ for the main lobe noise of the signal in BPSK modulation is [11]:

$$\delta\widetilde{\varphi}_{BPSK,main}(f) = 2\sqrt{2} \cdot \frac{\widetilde{A}_{BPSK}(f, f_{het})}{A_{het,rms}} \tag{3}$$

In Equation (3), $\widetilde{A}_{BPSK}(f, f_{het})$ can be expressed as:

$$\widetilde{A}_{BPSK}(f, f_{het}) = \sqrt{\frac{\left(A_{het,rms} \cdot m_{prn}\right)^2}{2f_{chip}} \cdot \mathrm{sinc}^2\left(\frac{|f - f_{het}|}{f_{chip}}\right)} \tag{4}$$

$f_{chip}$ represents the chip rate of the PRN code and $\mathrm{sinc}(x)$ is:

$$\mathrm{sinc}(x) = \begin{cases} 1, & x = 0 \\ \sin(\pi x)/(\pi x), & x \neq 0 \end{cases} \tag{5}$$

Thus, the estimation model for the main lobe noise $\delta\widetilde{\varphi}_{BPSK,main}(f)$ can be expressed as:

$$\delta\widetilde{\varphi}_{BPSK,main}(f) = 2\frac{m_{prn}}{\sqrt{f_{chip}}} \cdot \mathrm{sinc}(\frac{f}{f_{chip}}) \tag{6}$$

Secondly, the estimation model for the sidelobe phase noise $\delta\widetilde{\varphi}_{BPSK,side}(f)$ caused by BPSK modulation is given as [11]:

$$\begin{aligned}\delta\widetilde{\varphi}_{BPSK,side}(f) &= 2\frac{J_0^2(m_{sb})}{J_1^2(m_{sb})} \cdot \frac{m_{prn}}{\sqrt{f_{chip}}} \cdot \mathrm{sinc}(\frac{f+\Delta f_{sb}}{f_{chip}}) \\ &\approx 0 if\ f \ll \Delta f_{sb}\ and\ f_{chip} = \Delta f_{sb}\end{aligned} \tag{7}$$

$\Delta f_{sb}$ represents the frequency offset from the sidelobe to the main lobe.

From Equation (6), it can be seen that the main lobe noise is related to its modulation index and the PRN code chip rate. Taking the source coding design of LISA as an example, $m_{prn}$ is 0.1 rad, and $f_{chip}$ is 1.6 MHz [11]. Substituting into Equation (6), and considering $\mathrm{sinc}(\frac{f}{f_{chip}}) = 1$ (In the context of gravitational wave detection, the frequency band of interest ranges from $10^{-3}$ Hz to 1 Hz, meaning $f \ll f_{chip}$), the phase noise is approximately 158 μrad/$\sqrt{\mathrm{Hz}}$. This value is two orders of magnitude higher than the phase-tracking criterion for gravitational wave detection, which is 1 pm/$\sqrt{\mathrm{Hz}}$ (about 5.9 μrad/$\sqrt{\mathrm{Hz}}$ under a laser wavelength of 1064 nm). Secondly, from Equation (7), it can be seen that the sidelobe noise depends on the PRN and clock sideband modulation parameters. In the case where $f \ll \Delta f_{sb}$ and $f_{chip} = \Delta f_{sb}$, the sidelobe noise is approximately 0, where $\Delta f_{sb}$ is in MHz. Since $f \ll \Delta f_{sb}$ is always satisfied, it is only necessary to ensure $f_{chip} = \Delta f_{sb}$ to eliminate the sidelobe noise. Therefore, eliminating the main lobe noise caused by BPSK modulation is key to achieving high-precision phase tracking, which is the main focus of this study.

## 3. BBC Code Design and Optimization

The analysis above shows that the main lobe noise caused by BPSK modulation exceeds the phase-tracking requirements for gravitational wave detection by two orders of magnitude, which will severely impact the phase tracking accuracy. According to its generation mechanism, the DC component produced by an unbalanced PRN code causes main lobe noise, thereby increasing internal interference within the system and affecting the phase extraction accuracy. Therefore, a design method for BBC sequences is proposed that ensures bit balance within any length of the PRN sequence during data encoding to eliminate the impact of the DC component.

### *3.1. BBC Design Method*

In spread spectrum communication, when data are encoded into a PRN sequence, the data rate is much lower than the PRN chip rate. Therefore, a single data bit is subjected to an XOR operation with multiple PRN chips, which together are referred to as a combining window. According to this principle, if the PRN codes within the combining window are balanced, meaning that the numbers of 1 s and −1 s are equal, a balance can be achieved. This eliminates the DC component during modulation. To obtain the BBC sequence, this paper considers the optimization design of three commonly used pseudo-random code sequences: m sequences, gold sequences, and Weil sequences. Among them, the m-sequence is generated by an n-stage feedback shift register, and its corresponding feedback polynomial can be expressed as [16]:

$$f(x) = c_0 + c_1 + c_2x^2 + \cdots + c_nx^n, c_0 = c_n = 1 \tag{8}$$

In the equation, $c_0$, $c_1$, $c_2$, etc., represent the feedback coefficients. $c_1$ and $c_n$ are set to 1, while the remaining feedback coefficients are determined by the feedback polynomial, taking values of either 0 or 1. A coefficient of 0 indicates no feedback and 1 indicates participation in feedback. Once the feedback coefficients are determined, the m-sequence is also fixed, with its period being $2^n - 1$. Furthermore, gold sequences are generated by selecting two m-sequences of the same length, ensuring good correlation properties between them [17].

The Weil code is based on an XOR combination of two Legendre sequences of the same length. These two Legendre sequences share the same characteristic expression but differ by a certain phase offset. By varying the phase offset, different Weil code sequences can be generated. The characteristic expression of the Weil code sequence is given as [18]:

$$W(k,w) = L(k) \oplus L((k+w)\mathrm{mod}N), k = 0,1,2,\ldots,N-1 \tag{9}$$

In the equation, mod refers to the modulo operation; $w$ is the phase difference between the two Legendre sequences; and $L$ is the Legendre sequence, with its characteristic expression given as:

$$L(k) = \begin{cases} 0, k = 0 \\ 1, k \neq 0, and \ \ there\ exists\ an\ integer\ x\ such\ that\ k = x^2 \mathrm{mod}N \\ 0, others \end{cases} \tag{10}$$

Since the BBC sequence design requires modification of the original PRN sequence, an initial screening of the three pseudocode sequences is performed based on their correlation properties. The pseudocode with the best correlation performance is selected as the base sequence for the subsequent optimization of the BBC sequence. According to the requirements for gravitational wave detection and BBC sequence design, the length of the PRN sequence is set to 1024. To obtain a sequence of the desired length, m-sequences and gold sequences are traversed by inserting $-1$ or 1, while for the Weil sequence, the nearest prime number to 1024, 1031, is used, and it is truncated using a 7-bit cycle.

The results are shown in Table 1 and Figure 2 (the obtained results have not been normalized). Table 1 compares the correlation performance values of the three sequences before and after processing, while Figure 2 provides a visual comparison of the correlation performance of each sequence after processing. When the sequences were not processed, the autocorrelation of the m-sequence ($-60.20$ dB) was significantly better than that of the other two sequences, and the cross-correlation was also relatively similar. After processing, the autocorrelation of the m-sequence shows significant changes, with its stability being weaker than that of the other two sequences. This will affect the performance of the sequence itself when designing the BBC sequence later. The transformation of the gold sequence before and after processing is minimal, but its self- and cross-correlation performance ($-21.12$ dB, $-22.25$ dB) is weaker than that of the Weil sequence ($-23.82$ dB, $-23.95$ dB). Additionally, the generation principle of the gold sequence results in fewer code families than that of the Weil sequence. Therefore, the Weil sequence is selected as the pseudocode sequence for the subsequent BBC design.

**Table 1.** Comparison of the correlations of the three sequences.

| PRN | Status | Code Length | Max Autocorrelation Sidelobe $E_{Acorr}$/dB | Max Cross-Correlation Sidelobe $E_{Ccorr}$/dB | Remarks |
|---|---|---|---|---|---|
| m (Polynomial coefficients (10, 3) and (10, 5, 4, 2)) | Original | 1023 | −60.20 | −20.38 | $E_{corr} = 20\log_{10}(\frac{\lvert a_{corr}\rvert}{N})$ [1] |
| | Traverse and insert −1 or 1 | 1024 | −23.30 | −21.03 | |
| gold (m-preferred pair polynomial coefficients (10, 3) and (10, 8, 3, 2)) | Original | 1023 | −24.21 | −23.94 | |
| | Traverse and insert −1 or 1 | 1024 | −21.12 | −22.25 | |
| Weil | Original | 1031 | −24.22 | −24.37 | |
| | Cyclic truncation to 7 bits | 1024 | −23.82 | −23.95 | |

[1] $E_{corr}$ represents the correlation value, and $N$ represents the length of the PRN sequence.

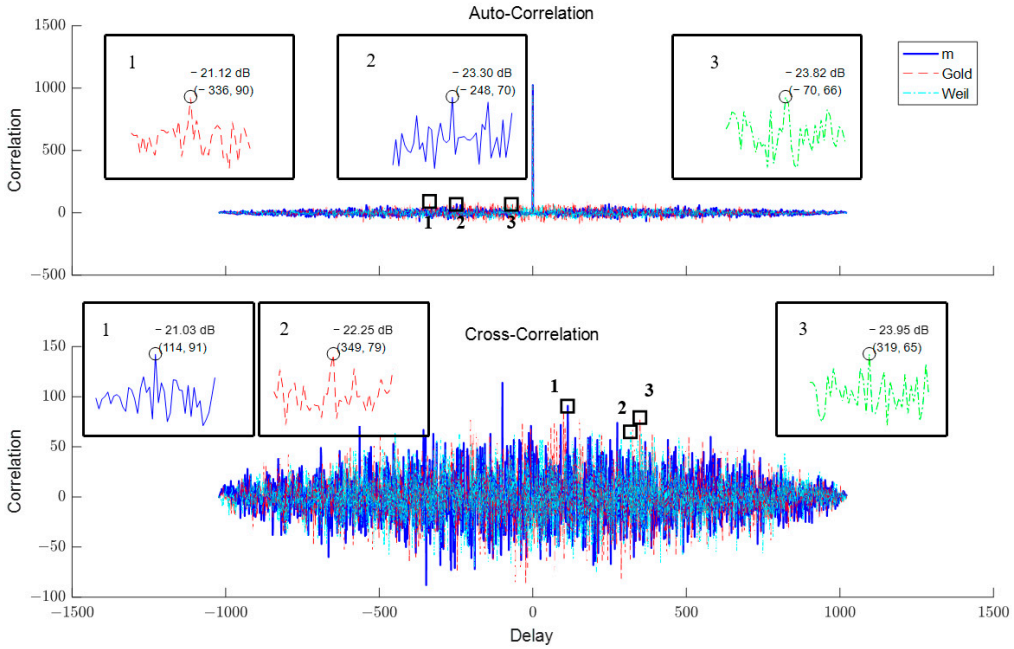


**Figure 2.** The maximum sidelobes of Autocorrelation and Cross-correlation for the three types of sequences.

The specific design process of the BBC sequence is shown in Figure 3.

1. Input parameters to select the order for generating PRN codes;
2. Generate a specified order of bipolar Weil sequence families based on the instructions;
3. Sequentially feed the pseudo-random sequences from the code family into the bit-balanced code design process until completion;
4. Group the input pseudo-random code sequences by every $n_{code}$ chips ($n_{code} = f_{chip}/f_{data}$, where $f_{data}$ is the data rate, representing the number of PRN codes corresponding to the combination window);
5. To minimize the disruption to the characteristics of the original pseudo-random code sequence, perform a preliminary screening of the PRN sequence groups segmented by $n_{code}$. The preliminary screening condition is that the absolute value of the sum of PRN chips in each group must be less than or equal to a variable $T_0 (T_0 = \lfloor n_{code}/10 \rfloor)$. If the condition is met, proceed to the next step; otherwise, discard the sequence and return to step 3;

6. For PRN sequences that meet the conditions, mark the indices of chips in each group that can be flipped;
7. Based on the sum $\pm T_0$ of the PRN chips in the group, randomly flip $|T_0|/2$ of the marked chips to make the sum equal to 0;
8. Reassemble the PRN sequences flipped by the group in step 7 into a new ranging PRN sequence in the order of their group numbers. This sequence is the bit-balanced code sequence, which is added to Set 1, and then returned to step 3.

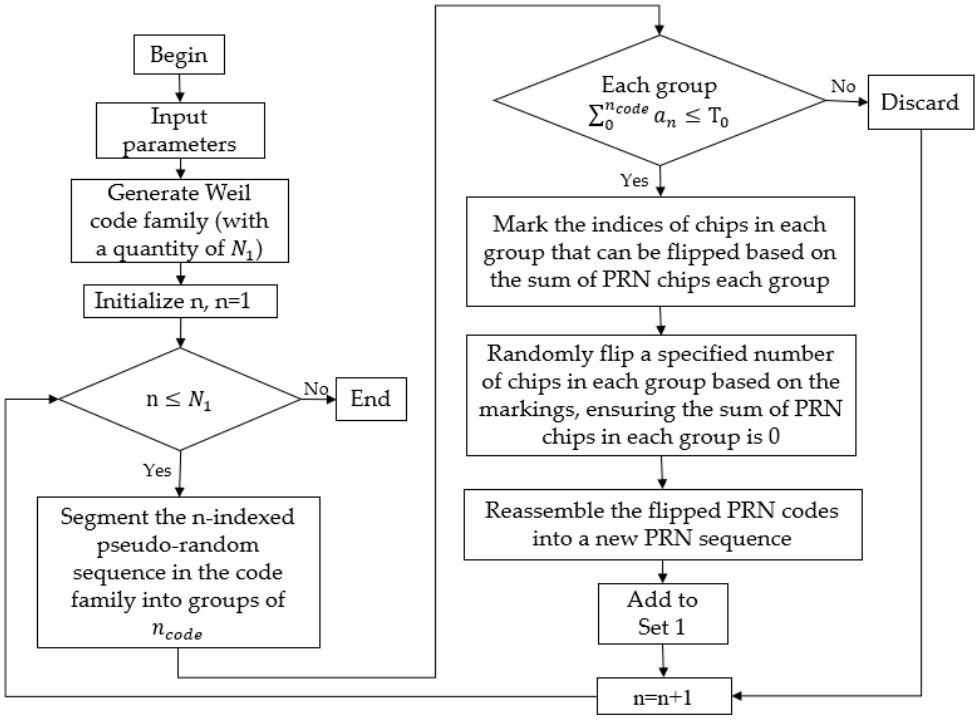


**Figure 3.** BBC design process.

### *3.2. BBC Optimization*

The BBC sequence family can be generated through the process described in Section 3.1. To select the best-performing BBC sequences, this paper conducts a comprehensive evaluation based on five indicators: odd/even autocorrelation, maximum spectrum amplitude, odd/even cross-correlation, and others. The definitions and computational complexities of these indicators are shown in Table 2.

**Table 2.** Preferred metrics and computational complexity.

| Evaluation Indicators | Definition | Computational Complexity | Computational Count |
|---|---|---|---|
| even autocorrelation | $R_{(a,a)}(\tau) = \sum_{i=0}^{N} a_i a_{i+\tau}$ | $O(N^2)$ | $M$ [2] |
| odd autocorrelation | $R_{(a,a)}(\tau) = \sum_{i=0}^{N-\tau-1} a_i a_{i+\tau} - \sum_{i=N-\tau}^{N-1} a_i a_{i+\tau}$ | $O(N^2)$ | $M$ |
| maximum spectrum amplitude | $Spec = \max\|FT(a(n))\|$ | $O(N\log_2(N))$ | $M$ |
| even cross-correlation | $R_{(a,b)}(\tau) = \sum_{i=0}^{N} a_i b_{i+\tau}$ [1] | $O(N^2)$ | $M(M-1)/2$ |
| odd cross-correlation | $R_{(a,b)}(\tau) = \sum_{i=0}^{N-\tau-1} a_i b_{i+\tau} - \sum_{i=N-\tau}^{N-1} a_i b_{i+\tau}$ | $O(N^2)$ | $M(M-1)/2$ |

[1] $a$ and $b$ represent PRN sequences, $\tau$ represents the chip shift value; [2] $M$ represents the number of codes in the code family.

When the length of the Weil sequence is 1024, the size of its code family reaches $1031 \times 1031$, indicating a significant computational burden for evaluating each indicator. Therefore, to reduce the computational burden, indicators other than cross-correlation are used for preliminary screening. Different weights are assigned to each indicator, and the average of the weighted sums of all indicators for each sequence in the code family is calculated. Screening is then performed based on $0.5\delta$ (standard deviation), as shown in Equation (11). Secondly, the odd/even cross-correlation indicator is used in the second step, applying the cross-correlation optimization method based on the maximum clique model, as shown in Equation (12). This method performs secondary screening on the candidate sequences obtained from the first step to derive the target number of BBC sequences with optimal performance.

$$\delta = \sqrt{\frac{1}{N}\sum_{i=1}^{N}(x_i - \mu)^2} \tag{11}$$

In the formula $x_i$ represents the data value, $\mu$ represents the overall mean.

$$R = \begin{bmatrix} 0 & d_{1,2} & d_{1,3} & d_{1,4} & \cdots & d_{1,n-1} & d_{1,n} \\ d_{1,2} & 0 & d_{2,3} & d_{2,4} & \cdots & d_{2,n-1} & d_{2,n} \\ d_{1,3} & d_{2,3} & 0 & d_{3,4} & \cdots & d_{3,n-1} & d_{3,n} \\ d_{1,4} & d_{2,4} & d_{3,4} & \ddots & \cdots & d_{4,n-1} & d_{4,n} \\ \vdots & \vdots & \vdots & \vdots & \ddots & \vdots & \vdots \\ d_{1,n-1} & d_{2,n-1} & d_{3,n-1} & d_{4,n-1} & \cdots & 0 & d_{n-1,n} \\ d_{1,n} & d_{2,n} & d_{3,n} & d_{4,n} & \ldots & d_{n-1,n} & 0 \end{bmatrix} \tag{12}$$

In the formula, $R$ is the cross-correlation performance matrix, where each PRN code is treated as a node, and the cross-correlation performance value $d_{a(n),b(n)}$ is considered as the distance between nodes. By setting a threshold to determine whether two nodes are connected, the target number of BBC sequences can be obtained.

The specific optimization process is shown in Figure 4.

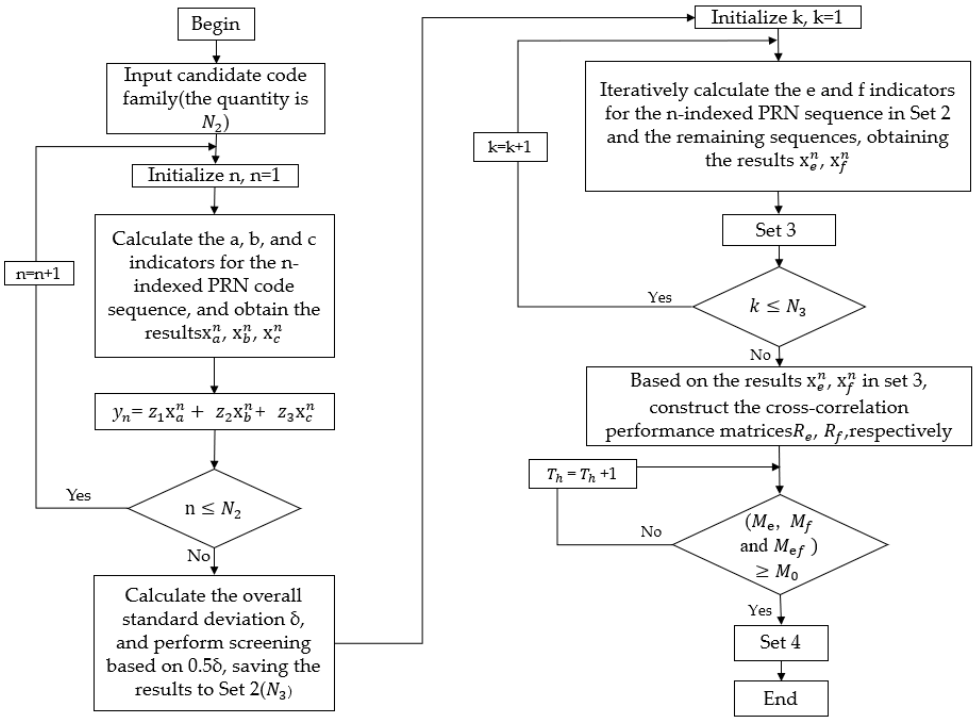


**Figure 4.** BBC optimization process.

1. Input the PRN code family designed with bit balance;
2. Sequentially input the PRN sequences from the code family into the loop to calculate the a, b, and ccc indicators for each sequence (a represents even autocorrelation, b represents odd autocorrelation, and c represents the maximum spectrum amplitude), obtaining the corresponding $x_a^n$, $x_b^n$ and $x_c^n$ values, until the process is complete;
3. Assign weights to the three indicators a, b and c, denoted as $z_1$, $z_2$ and $z_3$ ($z_1 + z_2 + z_3 = 1$). Calculate the total weighted sum $y_n$ of the three indicators for each sequence, and determine the overall standard deviation $\sigma$ of the code family. Filter the sequences using a threshold of $0.5\sigma$, and add those that meet the criteria to Set 2;
4. Iteratively calculate the e and f indicators for all pairs of PRN sequences in Set 2 (e represents even cross-correlation, and f represents odd cross-correlation), obtaining the corresponding $x_e^n$ and $x_f^n$ values, and store the results in Set 3;
5. Derive the cross-correlation performance matrices $R_e$ and $R_f$ for the code sequences in Set 3 based on the matrix definition in Equation (12);
6. Iteratively search through $R_e$ and $R_f$ matrices for $N_3 \times N_3$ elements, using their smallest non-zero value as the initial threshold $T_h$;
7. Apply the threshold $T_h$ to the $R_e$ and $R_f$ matrices to make decisions, obtaining the largest connected sets $A_e$ and $A_f$ with values not exceeding the threshold $T_h$, as well as their respective node counts $M_e$ and $M_f$;
8. Compare $M_e$ and $M_f$ with the target code count $M_0$. If they are smaller than $M_0$, the target requirement is not met. Increase the cross-correlation threshold by 1 and return to Step 8 for iteration. Repeat until $M_e \geq M_0$ and $M_f \geq M_0$, then exit the iteration;
9. Evaluate whether the number of matching node indices between $A_e$ and $A_f$ denoted as $M_{ef}$, meets the target code count $M_0$. If $M_{ef} < M_0$, the target requirement is not satisfied. Increase the cross-correlation threshold by 1 and return to Step 8 for iteration. Repeat until $M_{ef} \geq M_0$, then exit the iteration, add the results to Set 4, and terminate.

## 4. Simulation Experiment Comparison

To validate the effectiveness and reliability of the BBC design and optimization method, six sets of BBC sequences were generated and optimized using the parameters listed in Table 3. The system sampling frequency was set to 80 MHz, the PRN rate $f_{chip}$ was set to 1.6 MHz, the data code rate $f_{data}$ was set to 25 kbps, and the PRN code length was 1024. Under these settings, $n_{code} = 64$.

**Table 3.** Simulation of each index parameter.

| Type | Parameters | Value | Remarks |
|---|---|---|---|
| ranging communication system | system frequency $f_s$ | 80 MHz | Weil |
| | PRN rate $f_{chip}$ | 1.6 MHz | |
| | PRN length $N$ | 1024 | |
| | data rate $f_{data}$ | 25 Kbps | |
| BBC design | combination window $n_{code}$ | 64 | $n_{code} = f_{chip}/f_{data}$ |
| | variable $T_0$ | 6 | $T_0 = \lfloor n_{code}/10 \rfloor$ |
| BBC optimization | weight $z_1$, $z_2$, $z_3$ | 0.5, 0.25, 0.25 | $z_1 + z_2 + z_3 = 1$ |
| | PRN target code count $M_0$ | 6 | gravitational wave design requirements |

Six sets of BBC sequences were obtained using the parameters in Table 3, and their performance was compared with those of the original Weil sequences. The specific performance results for each indicator are shown in Figure 5 and Table 4. The maximum sidelobes of the correlation and maximum value ranges of the other indicators, along

with their averages, are presented (the mean is the actual data mean, not the center point of each range). It can be observed that the BBC sequences designed based on the Weil sequences, when compared to the original Weil sequences, show improved performance after optimization. Specifically, the mean value for the odd cross-correlation indicator remains the same as that of the original sequence at 95.33, while the average values for the even autocorrelation, odd autocorrelation, maximum spectrum amplitude, and even cross-correlation indicators are better than those of the original Weil sequence by 7.17, 2.83, 1.22, and 7.16, respectively. A comparison of various performance indicators shows that the BBC generation and optimization method can enhance the performance of the original sequence while modifying the balance and selecting the best-performing BBC sequences, thus verifying the effectiveness of this method.

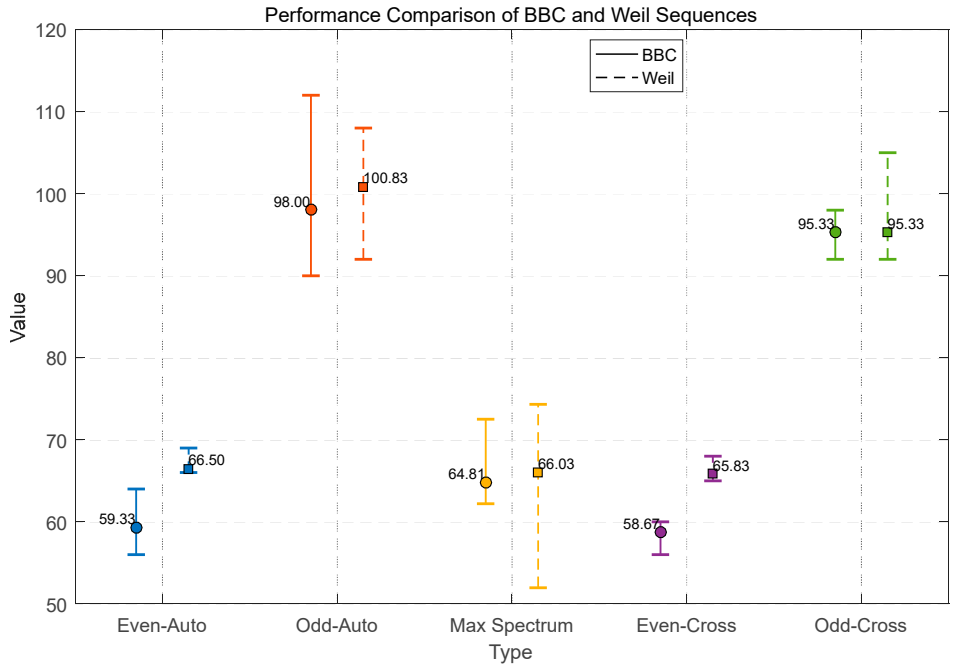


**Figure 5.** Performance comparison figure of BBC and Weil sequence.

**Table 4.** Performance Comparison Table of BBC and Weil Sequences.

| Type | Mean Even-Auto | Mean Odd-Auto | Mean Spectrum | Mean Even-Cross | Mean Odd-Cross |
|---|---|---|---|---|---|
| BBC | 59.33 | 98 | 64.81 | 58.67 | 95.33 |
| Weil | 65.50 | 100.83 | 66.03 | 65.83 | 95.33 |

Furthermore, to verify that the BBC sequences can effectively eliminate the DC component during BPSK modulation, random data were encoded into six optimized BBC sequences based on the parameters in Table 3, followed by cumulative mean statistics. The results are presented in Figure 6, which illustrates the cumulative mean before and after data encoding. For a balanced signal, the cumulative mean should approach zero. In the figure, the horizontal axis represents each sample point in the signal, while the vertical axis represents the cumulative mean at each sample point. The six optimized BBC sequences are depicted in blue and red, with solid lines representing BBC sequences without encoded data and dashed lines representing BBC sequences with encoded data. To enhance clarity, the encoded sequences are displayed with inversion. It can be observed that the BBC sequences exhibit consistent trends before and after encoding, with only minor fluctuations near zero. As the sample size increases, the mean rapidly converges to zero, indicating

that the sequences are globally balanced, with an average value approaching zero. This demonstrates that the BBC sequences are unaffected by random data, achieve dynamic bit balancing, and effectively eliminate the DC component.

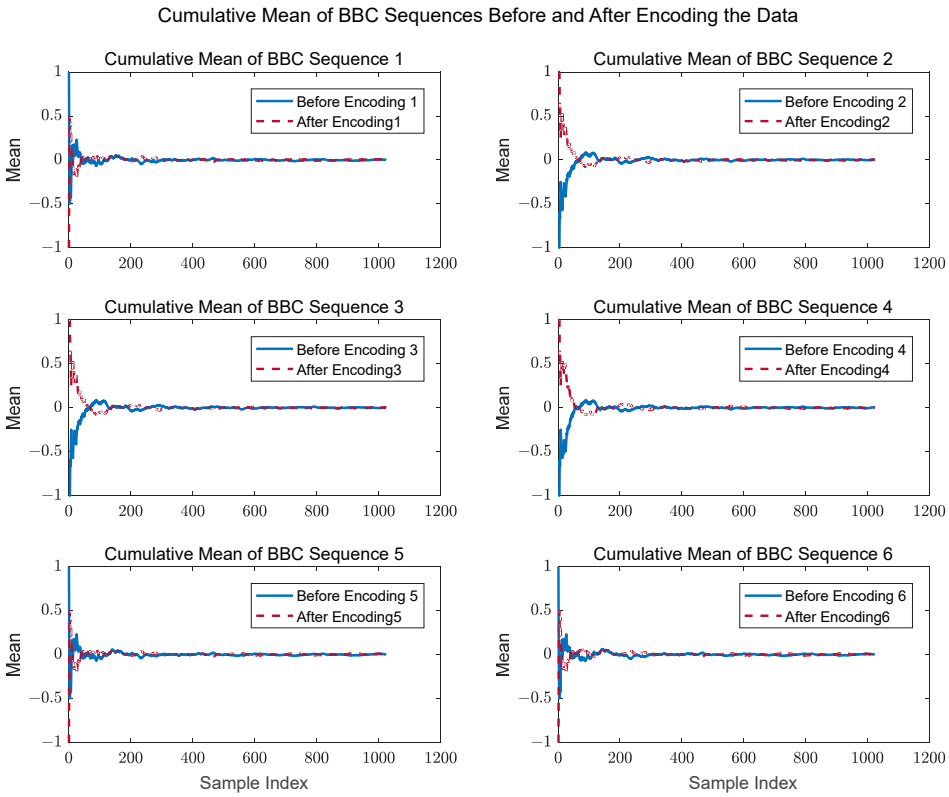


**Figure 6.** Comparison of BBC sequences before and after encoding the data.

## 5. Conclusions and Discussion

In the context of space gravitational wave detection, this paper analyzes the main lobe and sidelobe phase noise in a ranging communication system based on BPSK modulation. The study reveals that, due to the influence of the DC component, the main lobe phase noise under the current design specifications is approximately 158 $\mu rad/\sqrt{Hz}$, which is two orders of magnitude higher than the phase-tracking requirement of 5.9 $\mu rad/\sqrt{Hz}$. To eliminate the impact of main lobe noise, this paper proposes an optimized design method for BBC sequences and establishes a corresponding performance optimization system. The experimental results demonstrate that the optimized BBC sequences significantly outperform the original Weil sequences in four key metrics: even autocorrelation, odd autocorrelation, maximum spectrum amplitude, and even cross-correlation. The respective improvements are 7.17, 2.83, 1.22, and 7.16 on average. Furthermore, the experiments confirm that BBC sequences are immune to random data, achieve dynamic bit balancing, and effectively suppress DC components. In future research, the differences in actual inter-satellite communication environments can be further considered by incorporating complex channel conditions into experimental designs to comprehensively verify their robustness. Moreover, an in-depth study of the sidelobe noise in BPSK modulation is also of great significance, as it would provide broader technical support for space gravitational wave detection and other high-precision ranging communication applications.

**Author Contributions:** Methodology, H.L. and T.Y.; software, H.L.; validation, H.L., T.Y. and K.X.; writing—original draft preparation, H.L., T.Y., K.X. and Z.W.; writing—review and editing, H.L., T.Y.,

K.X. and Z.W.; visualization, H.L.; project administration, T.Y. and Z.W.; funding acquisition, T.Y. and Z.W. All authors have read and agreed to the published version of the manuscript.

**Funding:** This work was supported by the National Key R&D Program of China (2020YFC2200602), the National Key R&D Program of China (2020YFC2200604) and the National Key R&D Program of China (2020YFC2200600).

**Data Availability Statement:** The data presented in this study are not publicly available due to privacy, and access can be requested from [longhongyu@ciomp.ac.cn] upon reasonable request.

**Conflicts of Interest:** The author of the current study has no conflicts of interest to declare.

## References

1. Binetruy, P.; Bohe, A.; Caprini, C.; Dufaux, J.F. Cosmological backgrounds of gravitational waves and eLISA/NGO: Phase transitions, cosmic strings and other sources. *J. Cosmol. Astropart. Phys.* **2012**, *2012*, 027. [CrossRef]
2. Danzmann, K. LISA: Laser interferometer space antenna for gravitational wave measurements. *Class. Quantum Gravity* **1996**, *13*, A247. [CrossRef]
3. Luo, Z.R.; Bai, S.; Bian, X.; Chen, G.R.; Dong, P.; Dong, Y.H.; Gao, W.; Gong, X.F.; He, J.W.; Li, H.Y.; et al. Gravitational wave detection by space laser interferometry. *Adv. Mech.* **2013**, *43*, 415–447.
4. Delgado, J.J.E.; Marin, A.F.G.; Bykov, I.; Heinzel, G.; Danzmann, K. Free-Space Laser Ranging and Data Communication. In Proceedings of the 2009 6th Workshop on Positioning, Navigation and Communication, Hannover, Germany, 19 March 2009; IEEE: New York, NY, USA, 2009; pp. 275–281.
5. Gair, J.R.; Vallisneri, M.; Larson, S.L.; Baker, J.G. Testing general relativity with low-frequency, space-based gravitational-wave detectors. *Living Rev. Relativ.* **2013**, *16*, 1–109. [CrossRef] [PubMed]
6. Wang, Z.; Ma, J.; Li, J.Q. Space-based gravitational wave detection mission: Design highlights of LISA system. *Chin. Opt.* **2015**, *8*, 980–987. [CrossRef]
7. Tinto, M.; Dhurandhar, S.V. Time-delay interferometry. *Living Rev. Relativ.* **2014**, *17*, 1–54. [CrossRef] [PubMed]
8. MacWilliams, F.J.; Sloane, N.J. Pseudo-random sequences and arrays. *Proc. IEEE* **1976**, *64*, 1715–1729. [CrossRef]
9. Schwarze, T.S. *Phase Extraction for Laser Interferometry in Space: Phase Readout Schemes and Optical Testing*; TIB: Hannover, Germany, 2018.
10. Sweeney, D. *Laser Communications for LISA and the University of Florida LISA Interferometry Simulator*; University of Florida: Gainesville, FL, USA, 2012.
11. Yamamoto, K. *Intersatellite Clock Synchronization and Absolute Ranging for Gravitational Wave Detection in Space*; TIB: Hannover, Germany, 2023.
12. Esteban, J.J.; García, A.F.; Barke, S.; Peinado, A.M.; Cervantes, G.F.; Bykov, I.; Heinzel, G.; Danzmann, K. Experimental demonstration of weak-light laser ranging and data communication for LISA. *Opt. Express* **2011**, *19*, 15937–15946. [CrossRef] [PubMed]
13. Zhang, Y.B.; Deng, R.J.; Liu, H.S.; Luo, Z.R. Parameter Design and Experimental Verification of Taiji Program Inter-Satellite Laser Communication. *Chin. J. Lasers* **2023**, *50*, 2306002.
14. Deng, R.J.; Zhang, Y.B.; Liu, H.S.; Luo, Z.R. Ground electronics verification of inter-satellites laser ranging in the Taiji program. *Chin. Opt.* **2023**, *16*, 765–776.
15. Han, S. *Design and Implementation of Phasemeter Test System for Space Gravitational Wave Detection*; University of Chinese Academy of Sciences (Changchun Institute of Optics, Fine Mechanics and Physics, Chinese Academy of Sciences): Beijing, China, 2022.
16. Helleseth, T.; Li, C. An updated review on cross-correlation of m-sequences. *arXiv* **2024**, arXiv:2407.16072.
17. Xin, Y.Z. Analysis of M-Sequence and Gold-Sequence in CDMA System. In Proceedings of the 2011 IEEE 3rd International Conference on Communication Software and Networks, Xi'an, China, 27–29 May 2011; IEEE: New York, NY, USA, 2011; pp. 466–468.
18. Rushanan, J.J. Weil Sequences: A Family of Binary Sequences with Good Correlation Properties. In Proceedings of the 2006 IEEE International Symposium on Information Theory, Seattle, WA, USA, 9–14 July 2006; IEEE: New York, NY, USA, 2006; pp. 1648–1652.